Evaluating carbon sequestration efficiency in an ocean circulation model by adjoint sensitivity analysis

Chris Hill, Véronique Bugnion, Mick Follows, and John Marshall

Department of Earth, Atmospheric and Planetary Sciences, Massachusetts Institute of Technology, Cambridge, Massachusetts, USA

Received 14 August 2002; revised 22 May 2003; accepted 8 July 2004; published 10 November 2004.

[1] We demonstrate the application of the adjoint method to develop three-dimensional maps of carbon sequestration efficiency and mean residence time in an ocean general circulation model. In contrast to perturbation sensitivity experiments, the adjoint approach provides a computationally efficient way to characterize both temporal and spatial variations of sequestration efficiency and residence time for a complete global model domain. Sequestration efficiency (the percentage of carbon injected at a continuous point source that remains in the ocean after an elapsed time), for injections at the base of the main thermocline (~900 m), is initially lowest in the North Atlantic basin (except for regions of deep convection in the Labrador Sea) relative to the North Pacific. For injection periods of the order of a century or more, however, the model suggests that Pacific injection sites are generally less efficient for a constant rate injection source. The mean residence time (defined as the average period that impulsively injected carbon from a particular point source remains within the ocean) is also evaluated and mapped. This measure also suggests that Atlantic sequestration is more efficient in the long term. Our calculations draw out the dual role of convective mixing, both exposing shallow sequestration sources to the atmosphere and also, in the subpolar Atlantic and Labrador Sea, feeding carbon from shallow injection sources into the deep circulation away from the atmosphere. *INDEX TERMS:* 1635 Global Change: Oceans (4203); 4532 Oceanography: Physical: General circulation; 4806 Oceanography: Biological and Chemical: Carbon cycling; 3210 Mathematical Geophysics: Modeling; *KEYWORDS:* adjoint, ocean circulation, carbon sequestration

Citation: Hill, C., V. Bugnion, M. Follows, and J. Marshall (2004), Evaluating carbon sequestration efficiency in an ocean circulation model by adjoint sensitivity analysis, *J. Geophys. Res.*, *109*, C11005, doi:10.1029/2002JC001598.

1. Introduction

[2] Concern about the possible impact of fossil fuel CO_2 in the atmosphere has stimulated research into mitigation strategies. Sequestering fossil fuel CO_2 directly into the world's oceans has been proposed because, over the long term (hundreds to thousands of years), much fossil fuel CO_2 will be absorbed in to the large oceanic reservoir and will ultimately interact with the ocean sediments [see, e.g., *Archer and Maier-Reimer*, 1994]. Technologies have been explored in which CO_2 captured from concentrated sources such as power plants may be delivered directly into the deep ocean (reviewed by *Ormerod* [1996a, 1996b], *Ormerod and Angel* [1996a, 1996b], and *Caldeira et al.* [2001]) with a view to short-circuiting the atmospheric transient of CO_2 and reducing potential radiative and climatic impacts.

[3] For sequestration of carbon to be effective it must be injected at ocean sites for which the subsequent time before exposure to the atmosphere is long. Because the sequestration process itself requires the expenditure of additional energy it could ultimately be detrimental if sequestered carbon returns rapidly to surface waters where it may be transferred to the atmosphere [*Kheshgi et al.*, 1994]. It is critical to consider the nature of ocean circulation and tracer transports when evaluating the potential for long term carbon sequestration. Close to sites of injection, local currents, tides and bathymetry may play a significant role in setting the magnitude and persistence of near-field *pH* perturbations which could have immediate environmental impacts [*Caulfield et al.*, 1997a, 1997b; *Auerbach et al.*, 1997]. Large-scale ocean circulation and mixing processes are significant to long term sequestration efficiency. *Drange et al.* [2001] use a regional, isopycnal model of the North Atlantic to investigate the potential for sequestration of carbon from sources in the Norwegian Sea. They find that more than half of carbon injected from sources at depths of greater than 900 m is entrained into the model ocean's deep water circulation and retained in the ocean on timescales approaching a century and beyond. In addition there have been a number of global-scale studies using coarse resolution ocean circulation models, exploring the sensitivity of sequestration efficiency to injection site location [*Stegen et al.*, 1993; *Orr and Aumont*, 1999; *Orr et al.*, 2001; *Caldeira and Duffy*, 2000].

0148-0227/04/2002JC001598

[4] In this study we describe and illustrate the use of adjoint methods to evaluate the effectiveness of carbon sequestration as a function of injection site using the MIT general circulation model (MITgcm, http://mitgcm.org) [*Marshall et al.*, 1997a, 1997b].

[5] Recent studies have examined the sequestration efficiency of direct carbon injections in ocean circulation models with parameterized subgrid-scale ocean tracer transport and carbon cycle processes [*Stegen et al.*, 1993; *Orr and Aumont*, 1999; *Orr et al.*, 2001; *Caldeira et al.*, 2001]. These studies have used point-by-point perturbations of the model to compare the sequestration efficiency of a handful of injection locations by performing a series of numerical model simulations, one for each injection site, or with multiple tracers in one simulation. Such sensitivity tests provide only a partial picture of the model's sequestration characteristics. Moreover, developing a comprehensive global evaluation of efficiency through this direct approach is prohibitively expensive computationally, especially as model resolution increases.

[6] In recent years, highly efficient adjoint sensitivity methods have been applied to ocean circulation models to reveal the connections and sensitivities of ocean circulation and heat transports to surface boundary conditions and model parameterizations [*Marotzke et al.*, 1999; V. Bugnion and C. Hill, The equilibration of an adjoint model on climatological time scales, part i: Sensitivity of the thermohaline circulation to the surface boundary conditions, submitted to *Journal of Climate*, 2002 (hereinafter referred to as Bugnion and Hill, submitted manuscript, 2002a); V. Bugnion and C. Hill, The equilibration of an adjoint model on climatological time scales, part ii: The sensitivity of the thermohaline circulation to surface forcing and mixing in coupled and uncoupled models, submitted to Journal of Climate, 2002 (hereinafter referred to as Bugnion and Hill, submitted manuscript, 2002b). Such studies have been facilitated by the development and application of automatic differentiation tools applied to ocean circulation models [*Giering*, 1997; *Heimbach et al.*, 2002, 2004]. Here we apply a global configuration of the MIT ocean general circulation model and its adjoint to comprehensively map sequestration efficiency at very low computational cost, relative to the individual perturbation method. Using the adjoint sensitivity method we can evaluate the efficiency of sequestration for any injection site and for any time history of injection, out to thousands of years. The adjoint sensitivity example presented here computes the equivalent of more than 50,000 individual perturbation experiments in a single numerical integration, yet increases the computational cost by a factor of only 5 relative to a single perturbation experiment.

[7] It should be noted that while this technique presents an extremely efficient method for characterizing the regional and temporal variations of sequestration efficiency for a model, the inferences depend on the fidelity of the underlying numerical model configuration its parameterization of physical and biogeochemical processes and the boundary conditions employed. It is clear that the current generation of global ocean circulation and biogeochemistry models are not yet ready for predictive purposes. The ability of such models to simulate observed transient tracers (chlorofluorocarbons, CFCs) in the oceans, for example, has been discussed in detail by *Dutay et al.* [2001]. In a suite of global simulations using different global ocean circulation models, significant differences (both model-data and model-model) are seen in ocean CFC uptake and transport, attributable to differences in model subgrid-scale parameterizations, physical boundary conditions and unrepresented physical processes. Any conclusions drawn here should therefore be viewed as a thorough characterization of one such model rather than the real ocean.

[8] The paper is set out as follows: In section 2 we describe the MITgcm configuration used in this study and its representation of carbon from direct injection sources. In section 3 we outline measures which quantify the sensitivity of the air-sea flux of the injected carbon to individual source locations and illustrate how one proceeds with perturbation experiments. The adjoint method and its application to the optimal choice of injection site is described in section 4. In section 5 we discuss the adjoint solutions and conclude in section 6.

2. Ocean Circulation and Tracer Model

[9] We augment an MITgcm global ocean configuration [*Hill et al.*, 1995; *Marshall et al.*, 1997a, 1997b; *Adcroft et al.*, 1997; *Marshall et al.*, 1998; *Adcroft et al.*, 1999; *Hill et al.*, 1999] and its adjoint, described by *Marotzke et al.* [1999] and *Heimbach et al.* [2002] with a carbon-like tracer, C (see section 3). The circulation model is configured with lateral resolution of $4^\circ \times 4^\circ$ and realistic bathymetry with fifteen vertical levels (thicknesses 50 m near the surface to 690 m at depth). The transport due to subgrid-scale geostrophic eddies is parameterized as an eddy-induced velocity and isopycnal stirring according to *Gent and McWilliams* [1990]. Turbulent mixing in the surface boundary layer is represented by a convective adjustment scheme, homogenizing the water column where it is statically unstable. This configuration of the model, driven by surface heat, freshwater, and momentum fluxes from *DaSilva et al.* [1994], has been applied to climate sensitivity problems and is described in more detail by Bugnion and Hill (submitted manuscript, 2002a, 2002b).

[10] The circulation model is integrated to a steady state and forced by climatological wind stress, heat, and freshwater forcing. It broadly reproduces the expected large-scale features of the ocean general circulation (Figure 1). There are upper ocean wind-driven gyres, cyclonic in the Northern subpolar basins, anticyclonic in the subtropics. A circumpolar current in the Southern Oceans, transports 95 Sv through the Drake Passage. The upper ocean western boundary currents of the Gulf Stream and Kuroshio are clearly evident and well established.

[11] The thermohaline circulation is evident with deep water formation in the North Atlantic and deep western boundary currents. The steady state "residual mean" overturning stream function (the sum of the Eulerian mean and eddy velocities by which tracers are advected) is shown in Figure 2 for the global ocean. In the Northern Hemisphere the zonally averaged circulation is dominated by the 28 Sv North Atlantic overturning maximum centered around a depth of 1500 m and at a latitude of 58°N. Above 1000 m in the North Atlantic there is poleward flow. Beneath, around the level of the deep western boundary current (Figure 1), there is spreading of deep waters to the South. Strong sinking is evident in the band around 60°N. The overturning strength at 24°N is around 17 Sv. The over-

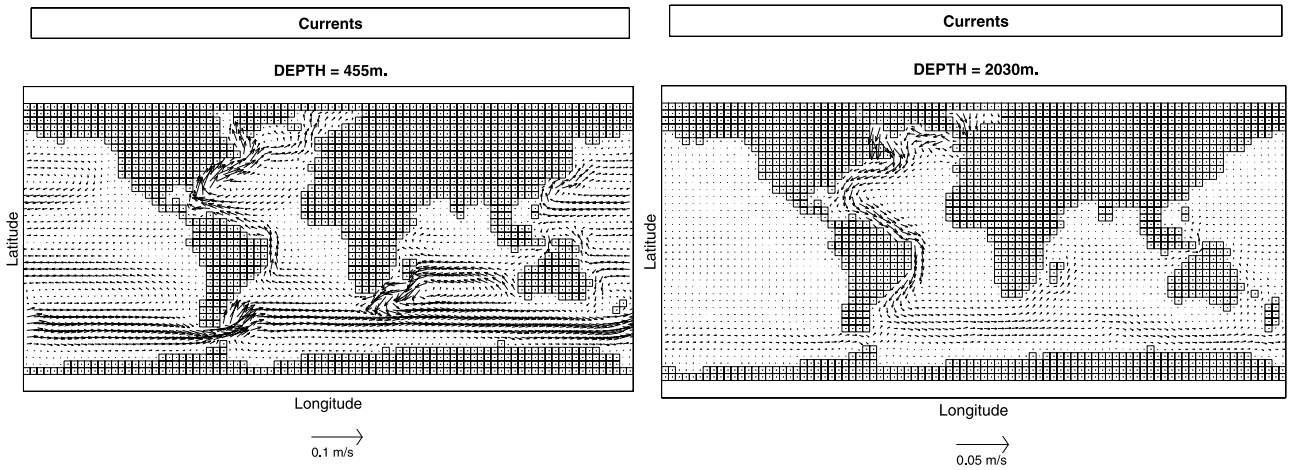

Figure 1. Ocean currents at a depth of 455 m and 2030 m (in m s^{-1} after 2000 years of spin-up).

turning numbers compare favorably to the inverse estimates of *Roemmich and Wunsch* [1985], *Macdonald and Wunsch* [1996], and *Ganachaud and Wunsch* [2000]. Details of the model's circulation depend upon the boundary conditions and particular parameter values and the sensitivities are discussed in detail by Bugnion and Hill (submitted manuscript, 2002a, 2002b). Aspects of a related model are examined by *Marotzke et al.* [1999] and by *Adcroft and Scott* [2001].

[12] We overlay on the ocean circulation model a parameterization of a carbon-like tracer, C. This tracer, described in detail in Appendix A, has the following properties: (1) It represents small deviations from the mean distribution of dissolved inorganic carbon in the ocean due to direct injection sources. (2) Away from the surface, C is transported by the models flow field and subgrid-scale mixing processes as a passive tracer in a manner identical to salinity. (3) C can have a point source at any or each ocean grid cell in the model. (4) The only sink of injected carbon-like tracer is loss to the atmosphere. (5) Source rates are assumed sufficiently small that the influence on atmospheric pCO_2 is negligible. Atmospheric pCO_2 is thus assumed uniform in space and time. There is no return transfer of injected carbon from the atmosphere to the ocean.

[13] Specifically, the injected carbon tracer, C, is governed by the prognostic equation:

$$\frac{\partial C}{\partial t} = -\vec{U} \cdot \nabla C + \nabla \cdot (K \nabla C) + \Gamma(C) - \mu C + S \qquad (1)$$

Within the ocean interior, the tracer is passively advected by model currents, $\vec{U}$, depicted in Figures 1 and 2. Isopycnal stirring is governed by the tensor K, transport during convective adjustment is represented by $\Gamma(C)$ and injection sources by S. In the surface layer of the model the carbon anomaly, C, is eroded by air-sea transfer parameterized as a decay with characteristic timescale $1/\mu \sim 1$ year (see Appendix A for scaling argument) consistent with the erosion of dissolved inorganic carbon anomalies by air-sea transfer at the ocean surface. In the interior of the ocean $\mu = 0$. Sequestration efficiency is sensitive to this timescale, relative to the surface residence time of water parcels, and more detailed, future studies should explore the sensitivity to this timescale.

[14] Our injected carbon tracer is analogous to that of the carbon injection experiments of *Orr et al.* [2001]. The

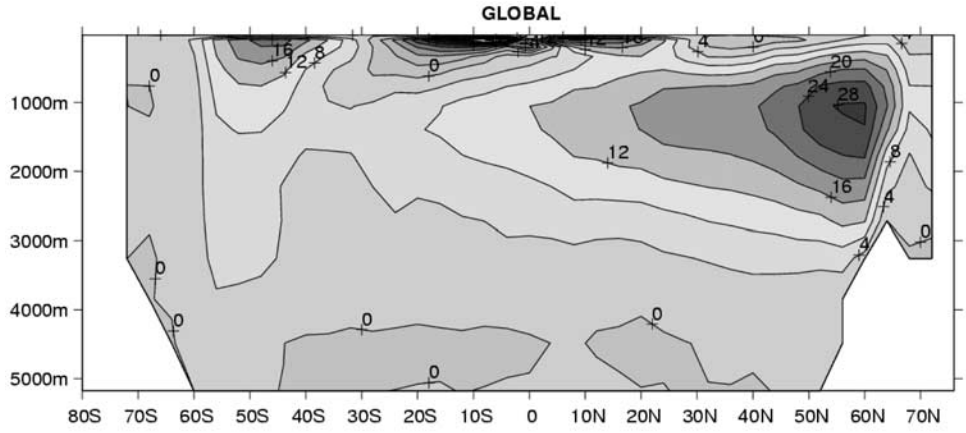

Figure 2. Meridional overturning, $\int_{z=-H}^{z=0} \int_{\lambda=\lambda_W}^{\lambda=\lambda_E} v d\lambda dz$ (in Sv after 2000 years of spin-up).

inferences concerning the sequestration efficiency of this idealized, "carbon-like" tracer, are valid in the limit where the strength of any individual source is small. For any individual injection source, this is likely be true. In practice, the emissions from a single source would be around 4×10^9 kg C year^{-1}. Over 100 years, such a pipeline would release 0.4 Gt C to the oceans. The current atmospheric burden of carbon dioxide is about 750 Gt C, so the 100 year emission from this single pipe, even if emitted directly in to the atmosphere, would change atmospheric pCO_2 by less than 0.05% (less than 0.2 ppmv) which is small relative to the annual cycle of a few ppmv at Mauna Loa. Hence we assume that this approach is valid for any single injection source, and that air-sea fluxes may be simply represented by the decay term $-\mu C$ in equation (1). However, in practice, there would be many such sources and the atmospheric build up could 'push back' on the ocean reducing outgassing. Future studies of significant sources such as this will need to use fuller descriptions of the ocean-atmosphere carbon system. Here, however, we focus on small perturbations and low source strengths.

3. Sensitivity Analysis

[15] To quantify and understand outgassing due to injections of C in equation (1), we calculate a scalar output or "cost function", J, of the model that measures the total amount of C lost by outgassing across the sea surface:

$$J(t=T) = \int_{t=0}^{t=T} \int_A \mu C \Delta z dA dt \tag{2}$$

[16] Equation (2) integrates the outgassing term, μC, from (1) over the entire ocean surface area, A (with surface layer thickness Δz) accumulating the outgassing up to time, T. J represents the amount of CO_2 (in moles) that would be outgassed during the time interval T. On sufficiently long timescales, any carbon injected by the source, S, in (1), will be exposed to the sea surface and ultimately lost to the atmosphere, increasing $J(t)$. The rate at which $J(t)$ rises depends not only on the injection rate S, but also on the time taken until there has been significant sea surface exposure of the injected carbon anomaly, which is determined by ocean circulation and mixing processes.

[17] We define two useful parameters which measure the sensitivity of the integrated air-sea flux of injected carbon, J, to impulsive local injections of carbon, δC, and continuous local sources of injected carbon, S. For an impulsive injection δC into a volume of ocean V (a grid cell in the case of our ocean model) the sensitivity measure

$$\widetilde{C} = \frac{1}{V}\frac{\partial J}{\partial C}(\lambda, \phi, z, t) \tag{3}$$

describes the evolution of $J(t)$ following an impulsive injection (i.e., an injection which is a delta function in time). $\widetilde{C}$ is nondimensional and ranges between 0 and 1. It expresses the ratio of total (time integrated) outgassed moles of carbon to the total impulsively injected input moles of carbon, $\delta C \times V$. $\widetilde{C}$ is a function of both injection location (λ, ϕ, z) and the time elapsed since the impulse injection t.

[18] For a continuous injection source, S, into a volume of ocean, V, we define the sensitivity:

$$\widetilde{S} = \frac{1}{tV}\frac{\partial J}{\partial S}(\lambda, \phi, z, t) \tag{4}$$

$\widetilde{S}$ is also nondimensional and ranges between 0 and 1. It expresses the ratio of total (time integrated) outgassed moles of carbon to total (time integrated) input moles of carbon from the continuous injection source of rate S. Here too, $\widetilde{S}$ is a function of both injection location (λ, ϕ, z) and time elapsed since the initiation of injection, t.

[19] Both $\widetilde{C}$ and $\widetilde{S}$ can be used to discriminate between regions for which the circulation patterns lead to rapid outgassing of injected carbon-like tracer and those that result in effective ocean sequestration. Regions in which $\widetilde{C}$ and $\widetilde{S}$ rise rapidly are regions where $J(t)$, the total amount of outgassed carbon, increases rapidly following injection and are therefore poor candidate areas for sequestration. Conversely, regions where sensitivity remains low for extended periods of time may be viable sequestration regions.

[20] The sensitivity parameters $\widetilde{C}$ and $\widetilde{S}$ may be evaluated for individual source locations, using perturbation experiments, or for any grid point source, using the adjoint sensitivity method. We first discuss the former. Evaluation of $\widetilde{C}$ and $\widetilde{S}$ requires knowledge of $\frac{\partial J}{\partial C}$ and $\frac{\partial J}{\partial S}$ respectively. A common approach to determine these sensitivities is to use finite difference approximations

$$\frac{\partial J}{\partial C}(\lambda_p, \phi_p, z_p, t) \sim \frac{\Delta J(t)}{\Delta C(\lambda_p, \phi_p, z_p)} \tag{5}$$

$$\frac{\partial J}{\partial S}(\lambda_p, \phi_p, z_p, t) \sim \frac{\Delta J(t)}{\Delta S(\lambda_p, \phi_p, z_p)} \tag{6}$$

[21] Here the change in the cost function, ΔJ, is divided by a perturbation in a single parameter, applied at a location ($\lambda = \lambda_p$, $\phi = \phi_p$, $z = z_p$). The perturbation approach requires that (1) is separately integrated for each source location (λ_p, ϕ_p, z_p). In practical terms, this means one integration of the tracer model for each potential injection location.

3.1. Example of Explicit Perturbation Method

[22] Using the ocean circulation model with injected carbon parameterized according to equation (1) we first illustrate results from two explicit integrations with continuous injection sources located off the west and east coast of the continental United States at ($\lambda_p = 78°$W, $\phi_p = 38°$N) and ($\lambda_p = 124°$W, $\phi_p = 36°$N), each at a depth of 935 m. The model is initialized with $C = 0$ everywhere and the sources are applied to a volume of fluid V_p, such that the nominal carbon injection rate in both cases is $S \times V_p = 1$ mole s^{-1}. Figure 3 shows the resulting distributions of C at depths of 25 m and 2030 m after 200 years of continuous injection. After this interval, injected carbon has reached the surface in both cases, some outgassing has occurred, and J can be evaluated using equation (2).

[23] As described in Appendix A, equation (1) is a perturbation equation about an assumed equilibrium distribution of dissolved inorganic carbon. Thus we may treat the injection source S and the outgassing J as perturbations

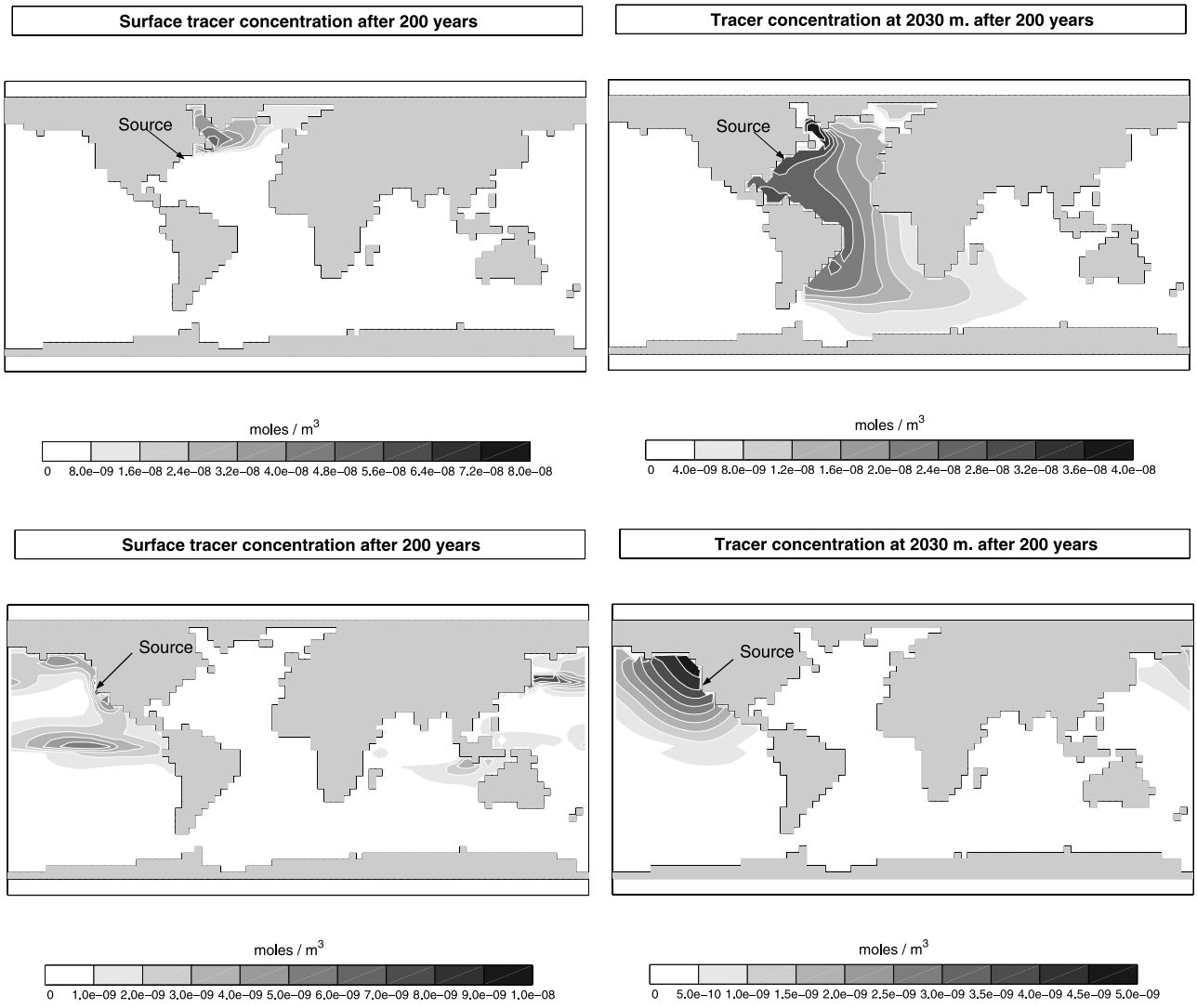

Figure 3. Tracer concentration after 200 years for two injection sites. Concentrations at (left) 25 m depth and (right) 2030 m depth are shown for injections at a depth of 935 m in the (top) Atlantic and (bottom) Pacific. At depth, tracer injected in the Atlantic is carried south by the deep western boundary current. Tracer is communicated to the surface at deep convection sites. Pacific injection is communicated to the surface along the equator, along the eastern boundary, and in the Kurishio region. At depth, Pacific tracer disperses isotropically away from the injection point.

about a reference state in which $S = 0$ and $J = 0$. Applying equation (6) we evaluate $\widetilde{S}$

$$\widetilde{S} = \frac{1}{tV_p}\left(\frac{\partial J}{\partial S}\right)_p = \frac{1}{tV_p}\left(\frac{J(t)}{S}\right)_p \tag{7}$$

for each injection point, denoted by the suffix p. For the North Atlantic source (Figure 3, top), after $t = 200$ years of continuous injection we find $J(t) = 1.2 \times 10^9$ moles and $\widetilde{S} = 0.2$, indicating that approximately 20% of the total tracer injected at that point, over the whole 200 year period, has outgassed. For the North Pacific (Figure 3, bottom) site $J(t) = 8.5 \times 10^8$ moles after 200 years and $\widetilde{S} = 0.14$, so approximately 14% of the injected carbon has outgassed.

[24] Thus, for these specific locations, source strengths and injection time, we find the Pacific source to be a more efficient sequestration site in this particular model. However, how do these results depend upon the locality of the injection sites? Perhaps if we moved each site by a few grid points (several hundred kilometers), or extended the analysis over a longer period of time, we would find the opposite to be true. Indeed, *Orr and Aumont* [1999] compared injection scenarios from different ocean models and found that the relative efficiency of Atlantic and Pacific injection sites was reversed between the two models. To what extent might this result have been due to small differences in local circulation and mixing patterns in each of the models or due to slightly different tim-dependent behavior in the two models? In order to address such questions it is very helpful to be able to map the sequestration efficiencies of all potential sources in such models. However, as is now discussed, this is prohibitively expensive using the perturbation method.

3.2. Computational Cost of the Perturbation Method

[25] The formulation of equation (1) as an anomaly equation avoids the need for a precursor ocean carbon

equilibration simulation. However, for each location ($\lambda = \lambda_p$, $\phi = \phi_p$, $z = z_p$) the perturbation approach requires that equation (1) be stepped forward separately. For a computational domain with longitudinal, latitudinal and vertical extents of N_x, N_y, N_z respectively, obtaining a complete map of sensitivities, for all points requires $\sim N_x N_y N_z$ simulations of length t; even at course resolution (4° lat/lon, as here) that is of the order of 60,000 simulations (somewhat less if continental points are discounted), each of 1000 years duration. Each simulation has a computational cost proportional to $N_x N_y N_z$. At the resolutions needed to even broadly represent the major ocean currents this number becomes prohibitive.

4. Adjoint Sensitivity

[26] Here we describe how to use the adjoint of our forward ocean model to provide a comprehensive and computationally efficient evaluation of the model's sensitivities. The application of the adjoint method to ocean models has been facilitated, in part, by the automatic differentiation of numerical models with the tangent linear adjoint model compiler of *Giering* [1997] and *Heimbach et al.* [2002, 2004]. Aided by this tool, the adjoint of the MIT ocean model has been obtained and applied to climate sensitivity studies by *Marotzke et al.* [1999] and Bugnion and Hill (submitted manuscript, 2002a, 2002b). The efficient evaluation of model sensitivities also lends itself to efficient optimization and state estimation techniques in which the ocean model is brought into consistency with observed data through systematic adjustment input parameters and boundary conditions [*Stammer et al.*, 2002]. Here we use the adjoint sensitivity method to evaluate the sequestration efficiency of the carbon-like tracer in this model.

[27] If a and b are model input variables, then the forward model, represented by the operator L in Figure 4, maps these on to the cost function J. The adjoint model, L^*, computes the adjoint variables (denoted by *) $a^* = \frac{\partial J}{\partial a}$, $b^* = \frac{\partial J}{\partial b}$. For example, the input variables might be the source S, or the advecting velocities, $\vec{U}$, or the impulsive injection, δC. Then the adjoint model yields the sensitivities:

$$S^*(\lambda, \phi, z, t) = \frac{\partial J}{\partial S}(\lambda, \phi, z, t) \tag{8}$$

$$C^*(\lambda, \phi, z, t) = \frac{\partial J}{\partial C}(\lambda, \phi, z, t) \tag{9}$$

$$\vec{U}^*(\lambda, \phi, z, t) = \frac{\partial J}{\partial \vec{U}}(\lambda, \phi, z, t) \tag{10}$$

at each point in the model at time t, which can be used to consider sequestration efficiency.

4.1. Adjoint Computational Cost

[28] The computational cost of the adjoint method scales linearly with the problem size $N_x N_y N_z$, and with simulation duration N_t in time steps. The adjoint model requires on the order of 5 times the computation of that of the forward. So, to infer sensitivities, over a 1000 year period, for each possible source in the model the total cost is equivalent to 5000 years of forward integration for the adjoint compared to tens of millions of years for the perturbation approach.

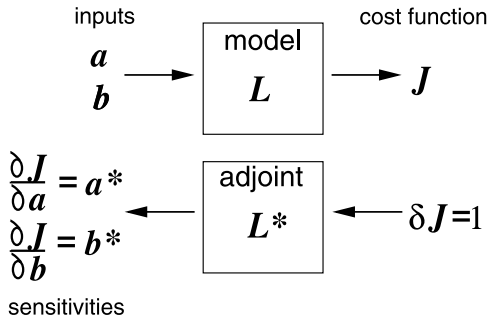

Figure 4. Schematic representation of the model-adjoint approach to estimation of sensitivities. The cost function J is evaluated as a function of the state of the forward model, **u**, which depends upon the input parameters a and b. The adjoint model works "in reverse" on a perturbation to the cost function to evaluate numerically the sensitivities of the cost function to the input parameters.

4.2. Testing the Adjoint Sensitivity

[29] The adjoint operator calculates the partial derivatives evaluated around a time-evolving but unperturbed model trajectory. In contrast the perturbation method calculates sensitivities by comparing a perturbed model trajectory with an unperturbed trajectory. For a nonlinear problem the answer calculated by the two methods can differ. However, for the linear advection/diffusion problem studied here, the adjoint and perturbation methods yield essentially the same result. Here we demonstrate this explicitly by a comparing the two methods.

[30] The adjoint of the ocean model and associated carbon model was constructed with the aid of the tangent linear adjoint model compiler of *Giering* [1997] and *Heimbach et al.* [2002, 2004]. The model-adjoint machinery was then used to evaluate the sensitivities $\widetilde{S}$ and $\widetilde{C}$ for sources at all ocean grid points in the model and out to 1000 years of model time. Figure 5 shows a time series of $\frac{\partial J}{\partial S}$ for a single point source, ($\lambda = 78°$W, $\phi = 38°$N, $z = 935$ m) calculated both with the explicit perturbation method, equation (6) (see section 3), and from the adjoint variable, S^*, in equation (8). The time-dependent sensitivities retrieved by the two methods for a single source location are almost identical. However, for a comparable computational cost, the adjoint experiment also evaluated S^* and C^* for all the other points in the model domain.

5. Analysis of Adjoint Sensitivity Results

[31] We now describe and discuss in more depth the comprehensive analysis of sequestration efficiency for the carbon-like tracer made possible by the adjoint method.

5.1. Efficiency and Mean Residence Time

[32] We consider two quantities relevant to the injected carbon tracer: The sequestration efficiency, E, and the mean residence time, $\overline{R}$. Sequestration efficiency is a function of time and location, and is defined as the percentage of injected carbon remaining in the ocean at time $t = T$. For

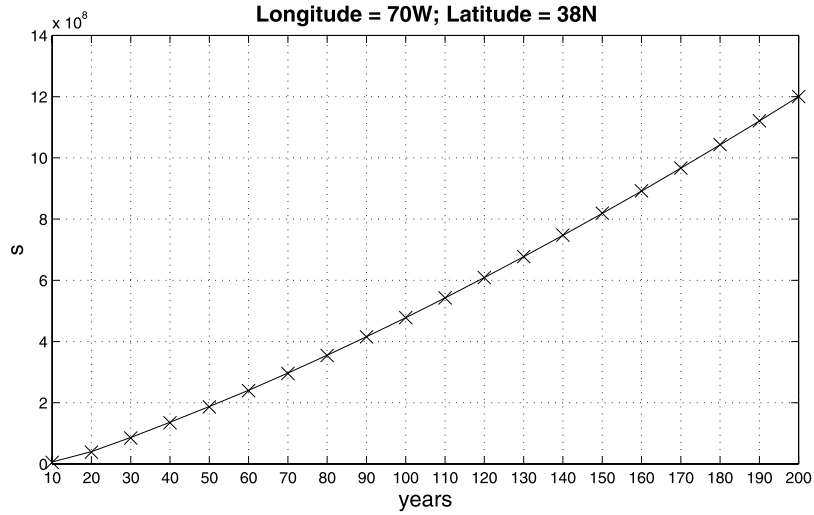

Figure 5. Perturbation and adjoint time series of sensitivity at a single point, (λ = 78°W, ϕ = 38°N, z = 935 m). The solid line is obtained using the adjoint method. Crosses are obtained from the perturbation approach.

a continuous, steady source, the efficiency at a particular time can be derived from $\widetilde{S}$ according to

$$E(t=T) = 100 \cdot \left(1 - \widetilde{S}(t=T)\right) \tag{11}$$

[33] Mean residence time, $\overline{R}$, is a measure of the average time tracer (carbon), from an impulsive injection (i.e., delta function in time), resides in the ocean before being lost to the atmosphere. Following the injection, some molecules may be rapidly exchanged, while others might persist in the ocean for a long time. $\overline{R}$ measures the mean residence time of the wide spectrum experienced by individual molecules. It is defined for an impulsive source and can be calculated from $\widetilde{C}$, evaluated for a unit impulse. Defining residence (the fraction of the impulsive injection remaining in the ocean at time $t = T$), R, as

$$R(t=T) = 1 - \widetilde{C}(t=T) \tag{12}$$

mean residence time is then given by

$$\overline{R} = \int_{t=0}^{t=T_f} R(t)dt = \int_{t=0}^{t=T_f} \left(1 - \widetilde{C}(t)\right)dt \tag{13}$$

where T_f is the time at which R falls to zero. Because R cannot fall below zero, $t = T_f$ is equivalent to $t = \infty$ in equation (13). While efficiency and residence vary with both space and time, the mean residence time is only a function of location.

[34] Using the adjoint approach we have evaluated both continuous source sensitivity, S^*, and impulsive source sensitivity, C^*, for up to one thousand years. Here we analyze the results in terms of efficiency, E, and mean residence time $\overline{R}$.

5.2. Efficiency: Sensitivity to Continuous Injection

[35] Efficiency is a function of both space and time. Figure 6 shows global maps of efficiency for sources at 935 m depth at three particular times following the onset of continuous injection (100 years, 500 years and 1000 years). Here we emphasize the time dependent nature of the basin to basin contrast in efficiency of sequestration of the injected tracer.

[36] The efficiency maps the amount of injected carbon from each site (i.e., each model grid point) which has been lost to the atmosphere, relative to the cumulative injection at that site. After 100 years of injection, in both Atlantic and Pacific basins, total efficiency remains quite high. The North Atlantic basin generally exhibits the lowest efficiencies at middepth, 935 m, with the exception of a small region in the Labrador Sea. The global maps made possible by the adjoint method allows us to clearly relate the efficiencies to ocean circulation processes. The low Atlantic efficiencies are consistent with waters at the base of the ventilated thermocline being upwelled at the western margin, returned to the surface and exposed to the atmosphere during deep winter mixing in the subpolar and northern subtropical gyres. The gyre is ventilated on decadal timescales, providing a pathway by which deeper thermocline waters can be drawn up to the surface and exposed to the atmosphere for long periods. In contrast in the Labrador Sea, a region of deep water formation in this model, a significant fraction of the carbon injected there finds its way into the abyssal ocean leading to high sequestration efficiencies. The weak overturning circulation and large gyres of the North Pacific make it (on the centennial timescale) a more efficient region for sequestration at this depth.

[37] After 500 years (and 1000 years) of injection, the contrast between the basins is reversed. On the longer timescale (still with continuous injection) the global overturning circulation has a stronger influence. While the efficiencies are reduced almost everywhere relative to the 100 year map, the Pacific, in the upwelling branch on the global overturning circulation, is a less efficient sequestration agent than the Atlantic, where deep waters are formed. Notably, the Labrador Sea is still a very efficient sequestration site due to its efficient connection to the abyss through the convective process. We note that

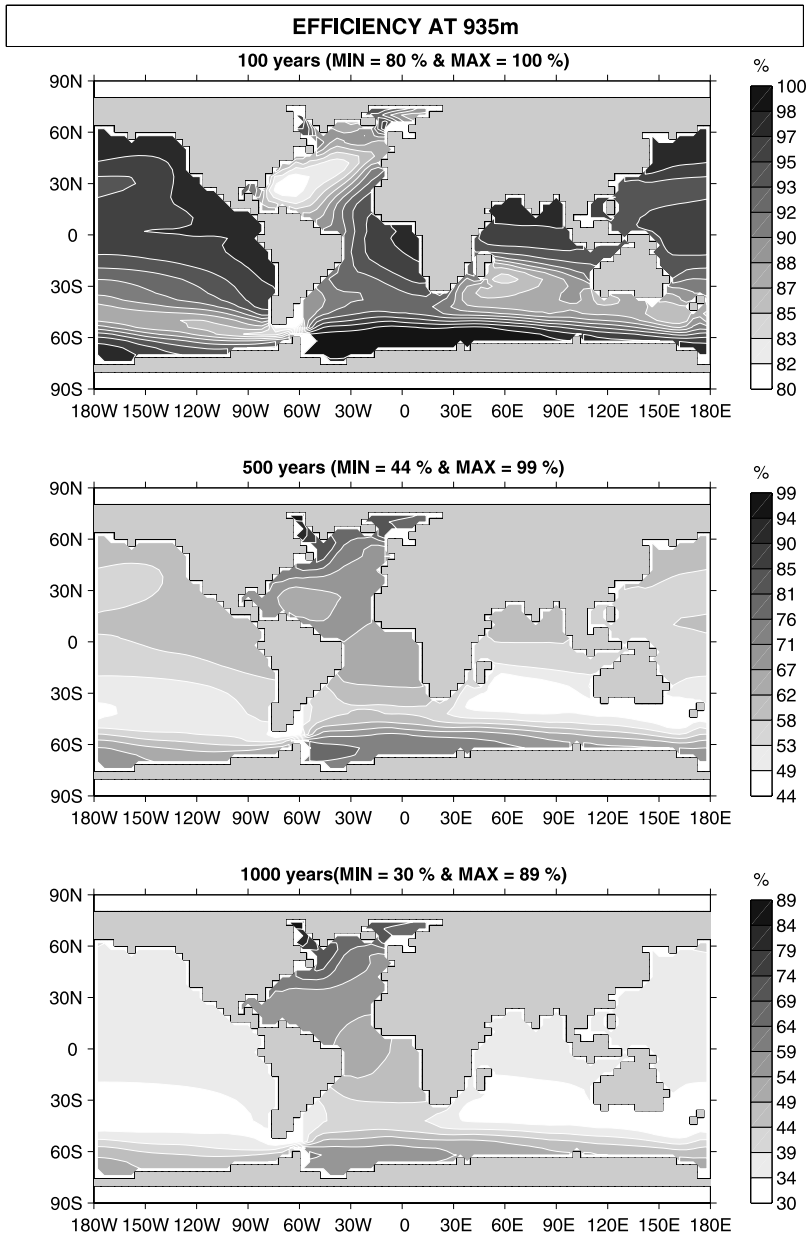

Figure 6. Sequestration efficiency, E, mapped as a function of latitude and longitude for continuous injection sources at 935 m in the ocean model at three time intervals (100, 500, and 1000 years) following the commencement of injection. The efficiency represents the percentage of total tracer, C, released at each grid cell during the time interval (at a constant source rate, S) that remains in the ocean at the end of the interval. These results were obtained using the adjoint model.

deep water formation occurs mainly in the Labrador sea in this, relatively coarse resolution, model. We note that the ocean, deep water formation can also occur in the Greenland sea (as is the case in the regional model of *Drange et al.*, 2001]. Since the convective process occurs on such small scales it is not well represented in coarse resolution models [*Marshall and Schott*, 1999] and is affected by the choice of subgrid-scale parameterizations [e.g., *Danabasoglu et al.*, 1994]. Hence the inferences from this specific model, while indicative of the important role of convective mixing regions, may not faithfully reproduce those that occur in nature.

[38] *Orr and Aumont* [1999], use the perturbation technique to evaluate model sequestration efficiencies and highlight an interesting contrast between two different global ocean models of carbon sequestration. They compare the efficiencies of sequestration between injection sites located near New York and Tokyo in each of the models, one suggesting the Atlantic as a more efficient sequester, the other the Pacific. The results shown here are not directly comparable, but clearly, they are model dependent. *Orr and Aumont* [1999] discuss model differences and suggest that model parameter choices, for example the coefficients of the subgrid-scale mixing parameterization, may lead to these

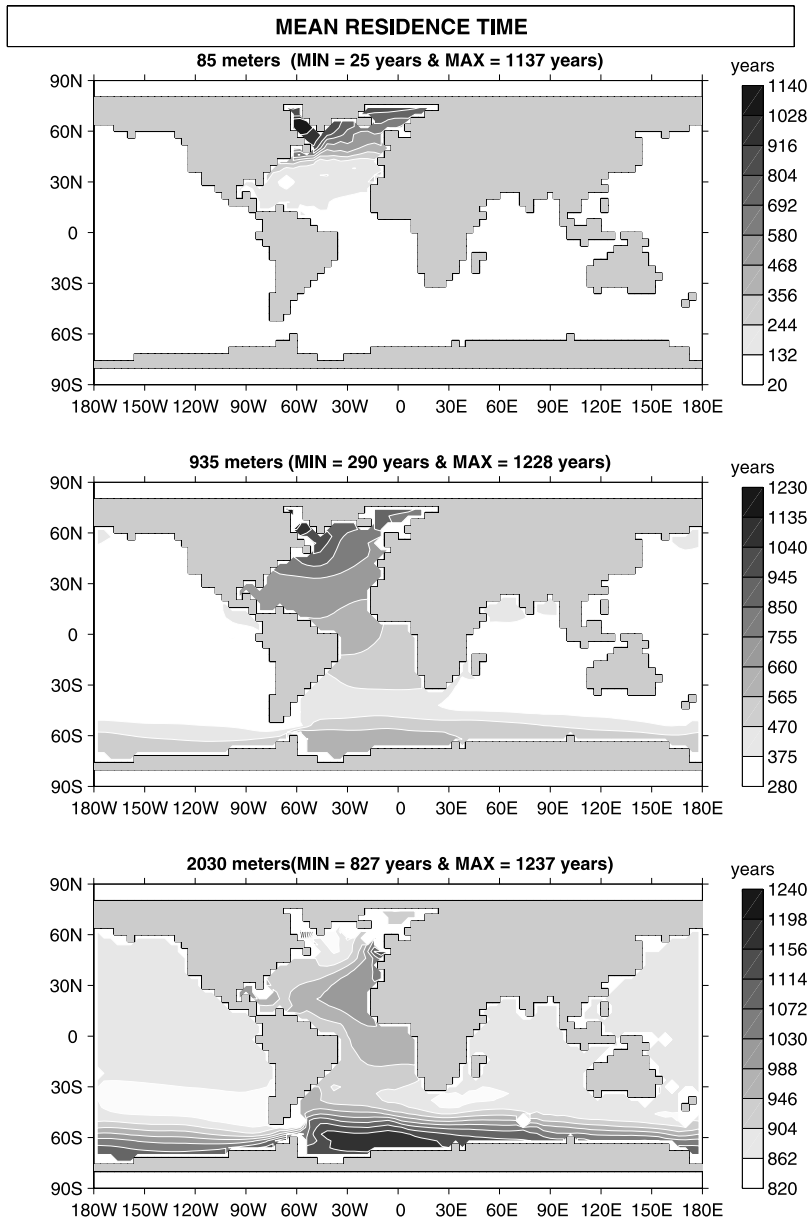

Figure 7. Mean residence time $\overline{R}$, mapped for continuous injection sources at three depth levels in the ocean model. $\overline{R}$ represents the mean time for an instantaneous pulse injection of tracer from that location to reside in the ocean before leaving across the air-sea interface.

different results. One way to examine such possibilities (although not done here) is to evaluate the sensitivities of the air-sea flux of injected carbon to mixing coefficient, or any such model parameter, using the adjoint method.

5.3. Mean Residence Time: Sensitivity to Impulsive Injection

[39] To evaluate $\overline{R}$, equation (13), we estimate T_f by extrapolation: the last three hundred years of $R(t)$ are extended using an exponential fit to estimate $R(t)$, $t >$ 1000 years and the time T_f at which residence approaches zero computed.

[40] Mean residence time, $\overline{R}$, is a function only of spatial location. In Figure 7 we show maps of $\overline{R}$ for depths of 85 m, 935 m and 2030 m. The residence times have been deduced by consideration of impulse injections. As would be expected, the mean residence time generally increases with depth of the source. In this model, the residence time of the carbon-like tracer injected at 2030 m is typically around 1000 years. For sources at 935 m the mean residence time is greater for the Atlantic basin where the deep waters originate, consistent with the long-time view from the efficiency (Figure 6). The basin to basin contrast is, however, relatively small. Typically, the 85 m sources show very short mean residence times, which is consistent with this level being within the seasonal boundary layer over much of the ocean, exposing the tracer quickly to the surface and loss to the atmosphere. However, in the North Atlantic where the model has very deep convection and deep water formation, convective mixing plays a different role. Now, a good deal of the tracer from the shallow injections is mixed deep into the ocean and carried away by the meridional overturning

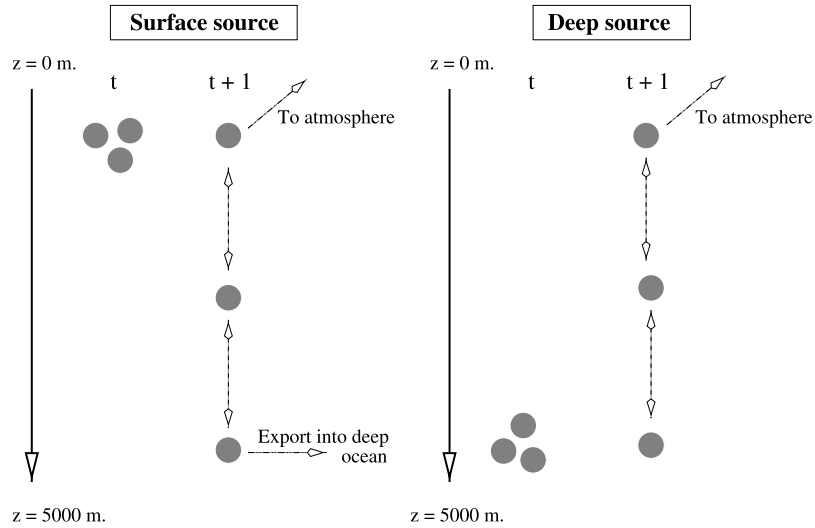

Figure 8. Schematic of the role of convection in dispersing carbon from injection sources during a time period t to $t + 1$. Relatively shallow injection sites can be efficient sequesters if placed close to convective mixing sites which rapidly transfer tracer away from the surface and to the abyss. In contrast, deep injection sources might be compromised if close to sites of convective mixing which could lead to the transport of carbon from depth to the surface and into contact with the atmosphere.

circulation, making the North Atlantic surface source mean residence time much longer than elsewhere in the upper ocean. This dual role for convective mixing is depicted schematically in Figure 8.

6. Discussion

[41] We have demonstrated the application of model-adjoint sensitivity analysis to study ocean carbon sequestration efficiency in an ocean model. The technique is extremely efficient, allowing a complete evaluation of sensitivity to source distribution at a computational expense comparable to a handful of individual, local source, perturbation experiments.

[42] We define ocean sequestration efficiencies (for continuous point sources) and mean residence time (for impulse injections) that can be derived from the sensitivities provided by the model and adjoint. These reveal that, for this model, the North Atlantic basin is more efficient at sequestering the tracer over timescales of several hundred years and longer. On shorter timescales however, for reasonable injection depths (about 1000 m) the Pacific basin is generally more efficient. Convective mixing plays a dual role; in the North Atlantic it mixes tracers from shallow injections into the deep ocean circulation, but elsewhere it exposes tracers to the atmosphere resulting in outgassing (see Figure 8). The maps produced by the adjoint method allow a clearer understanding of the regional differences in model sequestration efficiency in terms of oceanographic processes.

[43] The adjoint method can be easily applied to examine more closely the dependence of sequestration efficiency on physical parameters of the ocean model such as mixing coefficients or surface boundary conditions. Such studies may help to reveal the underlying mechanisms which lead to model-model discrepancies, as highlighted by *Orr and Aumont* [1999].

[44] The carbon-like tracer studied here provides some interesting insights and demonstrates the power and applicability of the adjoint method. However, it is important to remember that the inferences for carbon sequestration are valid only for sources of relatively small magnitude. If many such sources act in concert then the atmospheric push back becomes significant. Future studies should include a fuller description of the ocean-atmosphere carbon system to better account for such scenarios. Studies of the natural carbon cycle with the more detailed description will also very revealing of the regional and mechanistic controls on the air-sea fluxes of the unperturbed carbon carbon cycle.

[45] As a final note, it must be remembered that although this method is powerful in revealing the sensitivity characteristics of an ocean model, the insight gained into real ocean processes is always constrained by the veracity of the model under examination. In this demonstration of the method we have used a very coarse resolution, highly idealized model. Future studies should be undertaken at higher resolution, in order to more faithfully resolve the important boundary currents and even to resolve mesoscale eddy processes.

Appendix A: Injected Carbon Tracer

[46] Assume, following *Sarmiento et al.* [1992], that biological transformations of carbon are limited by other nutrients and that the efficiency of the ocean's biological pump of carbon is unaffected by small perturbations in dissolved inorganic carbon. Thus we assume that the carbon perturbations are simply a function of the solubility pump. Hence we will consider the prognostic equation for dissolved inorganic carbon (DIC) in an abiotic ocean model:

$$\frac{\partial \mathrm{DIC}}{\partial t} = -\vec{U} \cdot \nabla \mathrm{DIC} - \frac{V_p K_0}{h}\left(p\mathrm{CO}_2 - p\mathrm{CO}_2^{at}\right) + S \qquad \text{(A1)}$$

where the first term on the right represents the transport of carbon by the ocean circulation with velocity $\vec{U}$. This velocity is the sum of the Eulerian circulation and the eddy-induced velocity, parameterized with the scheme of *Gent and McWilliams* [1990]. The second term represents the air-sea exchange of CO_2 where pCO_2 is the partial pressure of dissolved CO_2 in surface waters; p^{at} the atmospheric partial pressure of CO_2; V_p is the air-sea gas transfer velocity; K_0 the temperature- and salinity-dependent solubility of CO_2, and h is the thickness of the surface mixed layer. Other sources and sinks of carbon, for example due to an anthropogenic injection, are represented by S.

[47] We represent the total carbon concentration as the sum of the natural background state, $\overline{C}$, and small perturbations around that state, C, due to the sources and sinks, S. Likewise p is the partial pressure at the surface associated only with the perturbation C. We assume here that pCO_2^{at} is constant, thus the perturbation carbon fluxes to the atmosphere must be small.

$$C = \overline{C} + C \qquad , \qquad pCO_2 = \overline{p} + p \tag{A2}$$

Hence

$$\frac{\partial(\overline{C}+C)}{\partial t} = -\vec{U}\cdot\nabla(\overline{C}+C) - \frac{V_p K_0}{h}(\overline{p}+p-p^{at}) + S \tag{A3}$$

For the unperturbed steady state, we may write

$$\frac{\partial \overline{C}}{\partial t} = -\vec{U}\cdot\nabla\overline{C} - \frac{V_p K_0}{h}(\overline{p}-p^{at}) = 0 \tag{A4}$$

Subtracting equation (A4) from equation (A3) we find the prognostic equation for the carbon anomaly associated with the source, S:

$$\frac{\partial C}{\partial t} = -\vec{U}\cdot\nabla C - \frac{V_p K_0}{h}p + S \tag{A5}$$

We relate small variations in p and C with a linear expansion,

$$p \simeq \frac{\partial p}{\partial C} C \tag{A6}$$

and infer from the Revelle, or Buffer factor [*Revelle and Suess*, 1957; *Bolin and Eriksson*, 1959]

$$B = \frac{\partial p / p^{at}}{\partial C / C^{eq}} \tag{A7}$$

where C^{eq} is the equilibrium dissolved inorganic carbon concentration at local temperature, salinity and p^{at}. Substituting from equations (A6) and (A7) into equation (A5), the air-sea exchange term may be approximated as a function of C.

$$\frac{V_p K_0}{h}p \;\sim\; \frac{V_p B}{h}\left(\frac{K_0 p^{at}}{C^{eq}}\right)C = \frac{V_p B}{h\alpha^{eq}}C \tag{A8}$$

where α^{eq} is the ionization fraction at equilibrium; the ratio of aqueous CO_2 to dissolved inorganic carbon [*Stumm and Morgan*, 1996]. $V_p B/h\alpha^{eq} = \mu\ (s^{-1})$ is a rate constant for the decay of carbon anomalies in the surface waters due to air-sea exchange [*McLaren and Williams*, 2001].

[48] Here we integrate the approximate prognostic equation (valid for small carbon perturbations)

$$\frac{\partial C}{\partial t} = -\vec{U}\cdot\nabla C - \mu C + S \tag{A9}$$

Typically, in today's ocean, $V_p \sim 5 \times 10^{-5}$ m s^{-1}, $B \sim 10$, $h \sim 100$ m, and $\alpha^{eq} \sim O(100)$, leading to the timescale for the erosion of the carbon anomalies at the surface, $1/\mu \sim 1$ year.

[49] **Acknowledgments.** We thank Eric Adams for helpful discussion and suggestions. JCM and MJF acknowledge support of the Ocean Carbon Sequestration Program, Biological and Environmental Research (BER), U.S. Department of Energy (grant DE-FG02-ER63017).

References

Adcroft, A., and J. R. Scott (2001), Impact of geothermal heating on global ocean circulation, *Geophys. Res. Lett.*, *28*(9), 1735–1738.

Adcroft, A. J., C. N. Hill, and J. Marshall (1997), Representation of topography by shaved cells in a height coordinate ocean model, *Mon. Weather Rev.*, *125*, 2293–2315.

Adcroft, A., C. Hill, and J. Marshall (1999), A new treatment of the Coriolis terms in C-grid models at both high and low resolutions, *Mon. Weather Rev.*, *127*, 1928–1936.

Archer, D., and E. Maier-Reimer (1994), Effect of deep-sea sedimentary calcite preservation on atmospheric CO_2 concentration, *Nature*, *367*, 260–264.

Auerbach, D. I., J. A. Caulfiled, E. E. Adams, and H. J. Herzog (1997), Impacts of ocean CO_2 disposal on marine life: I. A toxicological assessment integrating constant-concentration laboratory assay data with variable-concentration field exposure, *Environ. Model. Assess.*, *2*, 333–343.

Bolin, B., and E. Eriksson (1959), Changes in the carbon dioxide content of the atmosphere and the sea due to fossil fuel combustion, in *The Atmosphere and the Sea in Motion*, pp. 130–142, Rockefeller Inst. Press, New York.

Caldeira, K., and P. B. Duffy (2000), The role of the Southern Ocean in uptake and storage of anthropogenic carbon dioxide, *Science*, *287*, 620–622.

Caldeira, K., H. J. Herzog, and M. E. Wickett (2001), Predicting and evaluating the effectiveness of ocean carbon sequestration by direct injection, paper presented at First National Conference on Carbon Sequestration, Dep. of Energy, Washington, D. C.

Caulfield, J., D. Auerbach, E. E. Adams, and H. J. Herzog (1997a), Near field impacts of reduced pH from ocean CO_2 disposal, *Energy Conversion Manage.*, *38*, 343–348.

Caulfield, J., E. E. Adams, D. I. Auerbach, and H. J. Herzog (1997b), Impacts of ocean CO_2 disposal on marine life: II. Probabilistic plume exposure model used with a time-varying dose-response analysis, *Environ. Model. Assess.*, *2*, 345–353.

Danabasoglu, G., J. C. McWilliams, and P. R. Gent (1994), The role of mesoscale tracer transports in the global ocean circulation., *Science*, *264*, 1123–1126.

DaSilva, A. M., C. C. Young, and S. Levitus (1994), *Atlas of Surface Marine Data*, *NOAA Atlas NESDIS 7*, Natl. Oceanic and Atmos. Admin., Silver Spring, Md.

Drange, H., G. Alendal, and O. M. Johannsen (2001), Ocean release of fossil fuel CO_2: A case study, *Geophys. Res. Lett.*, *28*, 2637–2640.

Dutay, J.-C., et al. (2001), Evaluation of ocean model ventilation with CFC-11: Comparison of 13 global ocean models, *Ocean Model.*, *4*, 89–120.

Ganachaud, A., and C. Wunsch (2000), Improved estimates of global circulation, heat transport and mixing from hydrographic data, *Nature*, *408*, 453–456.

Gent, P. R., and J. C. McWilliams (1990), Isopycnal mixing in ocean circulation models, *J. Phys. Oceanogr.*, *20*, 150–155.

Giering, R. (1997), Tangent linear and adjoint model compiler, version 1.2 manual, Cent. for Global Sci., Mass. Inst. of Technol., Cambridge.

Heimbach, P., C. Hill, and R. Giering (2002), Automatic generation of efficient adjoint code for a parallel Navier-Stokes solver, *Lect. Notes Comput. Sci.*, *2330*, 1019–1028.

Heimbach, P., C. Hill, and R. Giering (2004), An efficient exact adjoint of the parallel MIT general circulation model, generated via automatic differentiation, *Future Generation Comput. Syst.*, in press.

Hill, C., A. Adcroft, D. Jamous, and J. Marshall (1999), A strategy for terascale climate modeling, in *Proceedings of the Eighth ECMWF Workshop on the Use of Parallel Processors in Meteorology*, pp. 406–425, World Sci., River Edge, N. J.

Kheshgi, H. S., B. P. Flannery, M. I. Hoffert, and A. G. Lapenis (1994), The effictiveness of marine CO_2 disposal, *Energy*, *19*, 967–975.

Macdonald, A., and C. Wunsch (1996), An estimation of global ocean circulation and heat fluxes, *Nature*, *382*, 436–440.

Marotzke, J., R. Giering, K. Q. Zhang, D. Stammer, C. Hill, and T. Lee (1999), Construction of the adjoint MIT ocean general circulation model and application to Atlantic heat transport sensitivity, *J. Geophys. Res.*, *104*(C12), 29,529–29,547.

Marshall, J., A. Adcroft, C. Hill, L. Perelman, and C. Heisey (1997a), A finite-volume, incompressible Navier Stokes model for studies of the ocean on parallel computers, *J. Geophys. Res.*, *102*(C3), 5753–5766.

Marshall, J., C. Hill, A. Adcroft, and L. Perelman (1997b), Hydrostatic, quasi-hydrostatic and non-hydrostatic ocean modeling, *J. Geophys. Res.*, *102*(C3), 5733–5752.

Marshall, J., H. Jones, and C. Hill (1998), Efficient ocean modeling using non-hydrostatic algorithms, *J. Mar. Syst.*, *18*, 115–134.

McLaren, A. J., and R. G. Williams (2001), Interannual variations in the thermodynamics of subduction over the North Atlantic, *J. Phys. Oceanogr.*, *31*, 3284–3294.

Ormerod, W. G. (1996a), *Ocean Storage of Carbon Dioxide. Workshop 1—Ocean Circulation*, IEA Greenhouse Gas R&D Programme (IEAGHG), London.

Ormerod, W. G. (1996b), *Ocean Storage of Carbon Dioxide. Workshop 3—International Links and Concerns*, IEA Greenhouse Gas R&D Programme (IEAGHG), London.

Ormerod, W. G., and M. Angel (1996a), *Ocean Storage of Carbon Dioxide. Workshop 2—Environmental Impact*, IEA Greenhouse Gas R&D Programme (IEAGHG), London.

Ormerod, W. G., and M. Angel (1996b), *Ocean Fertilisation as a CO2 Sequestration Option*, IEA Greenhouse Gas R&D Programme (IEAGHG), London.

Orr, J. C., and O. Aumont (1999), Exploring the capacity of the ocean to retain artificially sequestered CO_2, in *Greenhouse Gas Control Technologies*, pp. 281–286, Elsevier Sci., New York.

Orr, J. C., et al. (2001), Ocean CO_2 sequestration efficiency from 3-D ocean model comparison, in *Greenhouse Gas Control Technologies, Proceedings of the Fifth International Conference on Greenhouse Gas Control Technolgies*, pp. 469–474, CSIRO Publ., Collingwood, Australia.

Revelle, R., and H. E. Suess (1957), Carbon dioxide exchange between atmosphere and ocean and the question of an increase of atmospheric CO_2 during the past decades, *Tellus*, *9*, 18–27.

Roemmich, D., and C. Wunsch (1985), Two transatlantic sections: Meridional circulation and heat flux in the subtropical North Atlantic Ocean, *Deep Sea Res.*, *32*, 619–664.

Sarmiento, J. L., J. C. Orr, and U. Siegenthaler (1992), A perturbation simulation of CO_2 uptake in an ocean general circulation model, *J. Geophys. Res.*, *97*, 3621–3645.

Stammer, D., C. Wunsch, R. Giering, C. Eckert, P. Heimbach, J. Marotzke, A. Adcroft, C. N. Hill, and J. Marshall (2002), Global ocean circulation during 1992–1997, estimated from ocean observations and a general circulation model, *J. Geophys. Res.*, *107*(C9), 3118, doi:10.1029/2001JC000888.

Stegen, G. R., K. H. Cole, and R. Bacastow (1993), The influence of discharge depth and location on the sequestration of carbon dioxide, *Energy Conversion Manage.*, *34*, 857–864.

Stumm, W., and J. J. Morgan (1996), *Aquatic Chemistry, Chemical Equilibria and Rates in Natural Waters*, 3rd ed., 1022 pp., John Wiley, Hoboken, N. J.

V. Bugnion, M. Follows, C. Hill, and J. Marshall, Department of Earth, Atmospheric and Planetary Sciences, Massachusetts Institute of Technology, Cambridge, MA 02139, USA. (cnh@mit.edu)